Electronic Supporting Information for: Electron superhalogens as positronium superhalogens

Rafael Porras-Roldan[a], Felix Moncada[b], Jorge Charry[c], Marcio Varella[d], Roberto Flores-Moreno[e] and Andrés Reyes[a‡]

[a] *Department of Chemistry, Universidad Nacional de Colombia, Av. Cra 30 45-03, Bogotá, Colombia*

[b] *Department of Physics, AlbaNova University Center, Stockholm University, 106 91, Stockholm, Sweden.*

[c] *Department of Physics and Materials Science, University of Luxembourg, L-1511 Luxembourg City, Luxembourg*

[d] *Instituto de Física, Universidade de São Paulo, Rua do Matão 1731, 05508-090 São Paulo, Brazil*

[e] *Departamento de Química, Universidad de Guadalajara, Blvd. Marcelino García Barragán 1421, Col Olímpica, Guadalajara Jal., C.P. 44430, Mexico.*

‡ Corresponding author

email: areyesv@unal.edu.co

Contents

S1 Basis set preliminary studies

First, the impact of the electronic basis set (BS) selection was evaluated. The aug-cc-pVXZ (X=D,T,Q) electronic BS series was combined with the PSX-TZ BS for the positron. Results for LiF_2 and $MgCl_3$ are summarized in Table S1. The PAs and EAs calculated with the smaller DZ BS are within 0.1 eV of the results obtained with the larger TZ and QZ BS.

Table S1 Convergence test with respect to electronic basis set. All values in eV.

LiF_2	EA	PA	PsBE	$MgCl_3$	EA	PA	PsBE
DZ	5.75	3.71	2.66	DZ	5.70	2.91	1.81
TZ	5.77	3.78	2.75	TZ	5.71	2.97	1.88
QZ	5.82	3.80	2.82	QZ	-	2.99	-

Next, the impact of an additional positron BS centered on the metal atom was evaluated for four systems. This test was performed with the chosen aug-cc-pVDZ and PSX-TZ BS for electrons and positron respectively. The results are presented in Table S2). The impact of the additional positron BS on the PAs is almost negligible, as it increases the predictions only by 0.01-0.02 eV.

Table S2 Additional positron basis set test. All values in eV.

System	PA	PsBE	PA†	PsBE†
LiBr2	3.05	1.08	3.07	1.09
AlCl4	2.93	2.25	2.93	2.25
MgBr3	2.81	1.28	2.82	1.28
BBr4	3.03	1.32	3.04	1.32

† With additional positron BS centered on the metal atom.

Additionally, the impact of the electronic BS choice, from the aug-cc-pVXZ (X=D,T,Q) series, was evaluated for the LiF_2 EDA results. These calculations were performed with and without positron BS centered on the Li atom. The results are summarized on Table S3. These results reveal that the increase in the PA observed with the larger basis sets arises from the higher relative contribution of the correlation term.

Table S3 EDA contributions (in %) on PA[LiF_2^-] with respect to to electronic basis set and center of the positron BS.

	E_{Elec}	E_{Cor}	E_{Rlx}
DZ	90.7/90.8†	9.1/9.2†	0.2/0.2†
TZ	89.1/89.2†	10.6/10.7†	0.2/0.2†
QZ	88.6/88.7†	11.1/11.2†	0.2/0.2†

† With additional positron BS centered on the metal atom.

S2 VDE and Vertical PA

The vertical electron detachment energy of Y^- (VDE[Y^-]) corresponds to the process:

$$Y^-(r_{Y^-}) \rightarrow Y(r_{Y^-}) + e^- \qquad VDE[Y^-] = E[Y(r_{Y^-})] - E[Y^-(r_{Y^-})] \tag{1}$$

where r_{Y^-} denotes the optimized geometry of the anion.

Differences in the EA and vertical electron detachment values range from 0.54 to 3.05 eV and can be attributed to a significant geometric relaxation upon the release of an electron by the anion. A comparison between the optimized geometry of SH anions, summarized in Table 4 of the main document, and the neutral SH molecules, presented in Table S7 of the SI, reveals considerable changes in the M−X bond lengths and a reduction in symmetry in the neutral complex. Existing studies offer detailed information on the significant geometric relaxation after electron detachment in SH anions[1].

Vertical positron PA^v affinities follow:

$$PsY(r_{Y^-}) \rightarrow Y^-(r_{Y^-}) + e^+ \quad PA^v[Y^-] = E[Y^-(r_{Y^-})] - E[PsY(r_{Y^-})] \tag{2}$$

Vertical PsBE will be calculated as:

$$PsBE^v[Y] \ = VDE[Y^-] + PA^v[Y^-] - 6.8 \tag{3}$$

Results for VDE and PA^v are presented in Table S4.

Table S4 VDE/PA^v energies (in eV) of the MX_{k+1}^- systems.

X	LiX_2^-	BeX_3^-	BX_4^-		
F	6.72/3.71	8.29/3.59	9.10/3.54		
Cl	6.05/3.20	6.83/3.17	6.59/3.15		
Br	5.56/3.07	6.26/3.05	5.94/3.03		
X	NaX_2^-	MgX_3^-	AlX_4^-	SiX_5^-	PX_6^-
F	6.35/3.56	8.17/3.28	9.55/3.21	9.31/3.21	9.94/3.19
Cl	5.80/3.05	6.97/2.91	7.30/2.93	7.76/2.93	6.80/2.93
Br	5.46/2.89	6.46/2.81	6.60/2.84	5.85/2.84	6.08/2.85

Table S5 Vertical positronium binding energies of the MX_{k+1} SH systems estimated from Eq. (3) , at the MC-MP2/aug-cc-pVDZ/PSX-TZ level of theory. All values in eV.

X	LiX_2	BeX_3	BX_4		
F	3.63	5.08	5.84		
Cl	2.45	3.20	2.94		
Br	1.81	2.51	2.17		
X	NaX_2	MgX_3	AlX_4	SiX_5	PX_6
F	3.12	4.68	5.96	5.72	6.34
Cl	2.04	3.08	3.43	3.89	2.93
Br	1.56	2.47	2.64	1.89	2.13

S3 Partial charge analysis

Table S6 Total electrostatic charges (CHELPG ESP)

System	A	B	C	D
LiF2	0.822	−0.911	0.811	−0.906
NaF2	0.891	−0.949	0.898	−0.945
BeF3	1.219	−0.739	1.188	−0.729
MgF3	1.518	−0.840	1.503	−0.834
BF4	1.203	−0.551	1.144	−0.536
AlF4	1.511	−0.628	1.471	−0.618
SiF5	1.728	−0.521(ax)/−0.583(eq)	1.687	−0.578(eq)/−0.510(ax)
PF6	1.715	−0.453	1.660	−0.443
LiCl2	0.702	−0.851	0.672	−0.836
NaCl2	0.774	−0.887	0.770	−0.885
BeCl3	0.940	−0.647	0.882	−0.629
MgCl3	1.186	−0.730	1.144	−0.714
BCl4	0.850	−0.462	0.758	−0.440
AlCl4	0.958	−0.490	0.882	−0.470
SiCl5	1.052	−0.356(ax)/−0.493(eq)	0.981	−0.335(ax)/−0.487(eq)
PCl6	0.984	−0.331	0.905	−0.317
LiBr2	0.677	−0.839	0.637	−0.819
NaBr2	0.746	−0.872	0.736	−0.867
BeBr3	0.888	−0.629	0.823	−0.608
MgBr3	1.121	−0.707	1.071	−0.690
BBr4	0.834	−0.458	0.734	−0.433
AlBr4	0.894	−0.473	0.804	−0.451
SiBr5	0.989	−0.333(ax)/−0.495(eq)	0.913	−0.310(ax)/−0.491(eq)
PBr6	1.000	−0.333	0.916	−0.320

[A] Metal charge in MX_{k+1}^{-}
[B] Halogen charge in MX_{k+1}^{-}
[C] Metal charge in $PsMX_{k+1}$
[D] Halogen charge in $PsMX_{k+1}$

S4 Optimized geometries

Table S7 MP2/aug-cc-pVDZ optimized metal halogen distances in neutral MX_{k+1} systems

System	M-X1	M-X2	M-X3	M-X4	M-X5	M-X6
LiF2*	1.711	1.710	-	-	-	-
NaF2*	2.061	2.061	-	-	-	-
BeF3	1.423	1.423	2.098	-	-	-
MgF3	1.775	1.775	2.264	-	-	-
BF4	1.336	1.336	1.336	2.691	-	-
AlF4	1.667	1.667	1.667	1.667	2.189	-
SiF5	1.607	1.607	1.607	1.607	3.209	-
PF6	1.586(eq)	1.586(eq)	1.586(eq)	1.620(ax)	1.620(ax)	3.374
LiCl2*	2.203	2.202	-	-	-	-
NaCl2*	2.573	2.573	-	-	-	-
BeCl3	1.975	1.975	1.835	-	-	-
MgCl3	2.367	2.367	2.211	-	-	-
BCl4	1.786	1.786	1.943	1.943	-	-
AlCl4	2.113	2.113	2.270	2.270	-	-
SiCl5	2.064	2.054	2.051	2.051	3.837	-
PCl6	2.056(eq)	2.056(eq)	2.072(eq)	2.162(ax)	2.162(ax)	3.981
LiBr2*	2.370	2.370	-	-	-	-
NaBr2*	2.737	2.737	-	-	-	-
BeBr3	2.123	2.123	1.986	-	-	-
MgBr3	2.517	2.517	2.358	-	-	-
BBr4	2.002	2.002	2.002	2.002	-	-
AlBr4	2.268	2.268	2.428	2.428		-
SiBr5	2.234	2.213	2.213	2.218	3.944	-
PBr6	2.260(eq)	2.232(eq)	2.227(eq)	2.360(ax)	2.630(ax)	4.022

All values in Å

* $Li/NaMX_2$ systems lose the linear geometry forming an XMX angle different from 180

S5 Energy decomposition analysis

Table S8 EDA results for e^+SH anions complexes. Energy values in atomic units.

System	E_{elec}	E_{rlx}	E_{corr}	e^+BE
LiF2	0.123828	0.000274	0.012393	0.136495
NaF2	0.118896	0.000255	0.011613	0.130763
BeF3	0.117452	0.000180	0.014182	0.131814
MgF3	0.108691	0.000113	0.011808	0.120612
BF4	0.114242	0.000162	0.015585	0.129989
AlF4	0.105155	0.000108	0.012786	0.118050
SiF5	0.103533	0.000094	0.014324	0.117951
PF6	0.101811	0.000078	0.015418	0.117307
LiCl2	0.098663	0.000265	0.018697	0.117625
NaCl2	0.093922	0.000161	0.017912	0.111995
BeCl3	0.094543	0.000324	0.021724	0.116590
MgCl3	0.088028	0.000223	0.018824	0.107075
BCl4	0.091725	0.000236	0.023885	0.115846
AlCl4	0.086219	0.000231	0.021160	0.107609
SiCl5	0.084001	0.000166	0.023419	0.107586
PCl6	0.081761	0.000120	0.025834	0.107715
LiBr2	0.092535	0.000324	0.019412	0.112272
NaBr2	0.087764	0.000157	0.018382	0.106303
BeBr3	0.088723	0.000380	0.022934	0.112037
MgBr3	0.082900	0.000286	0.020075	0.103261
BBr4	0.085919	0.000265	0.025317	0.111501
AlBr4	0.081266	0.000277	0.022838	0.104382
SiBr5	0.078888	0.000572	0.023434	0.102894
PBr6	0.076375	0.000143	0.028164	0.104681

Additionally, we present in Fig S1 the relation between the E_{Elec} and the charge on the halogen atoms for the MX_{k+1}^- systems

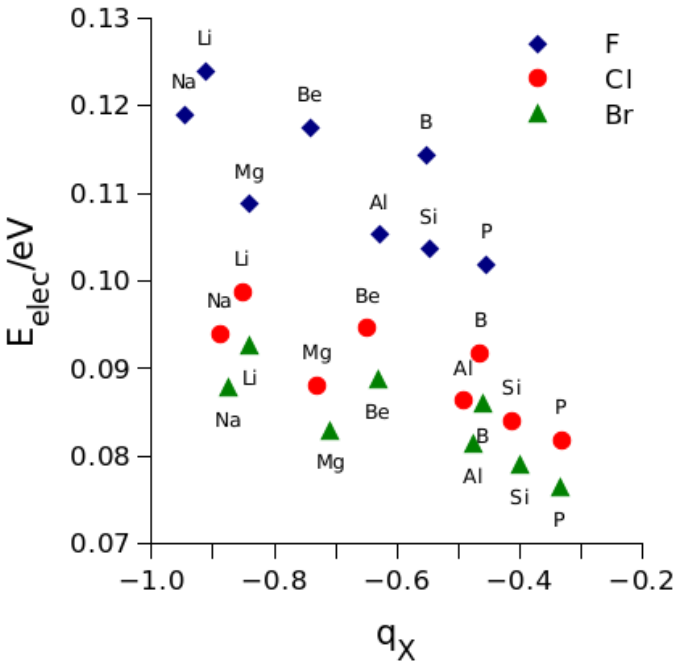

Figure S1 Total electrostatic charge (CHELPG ESP) on a halogen atom in MX_k^- compared to the electrostatic term of the PA energy decomposition.

S6 Electrostatic potential and positron density

We present plots (Figs. S2-S9) for total electrostatic potential (ESP) and positron density of MX_{k+1}^- and $PsMX_k$ respectively. Potential and density values in a.u, X and Y axis in Å.

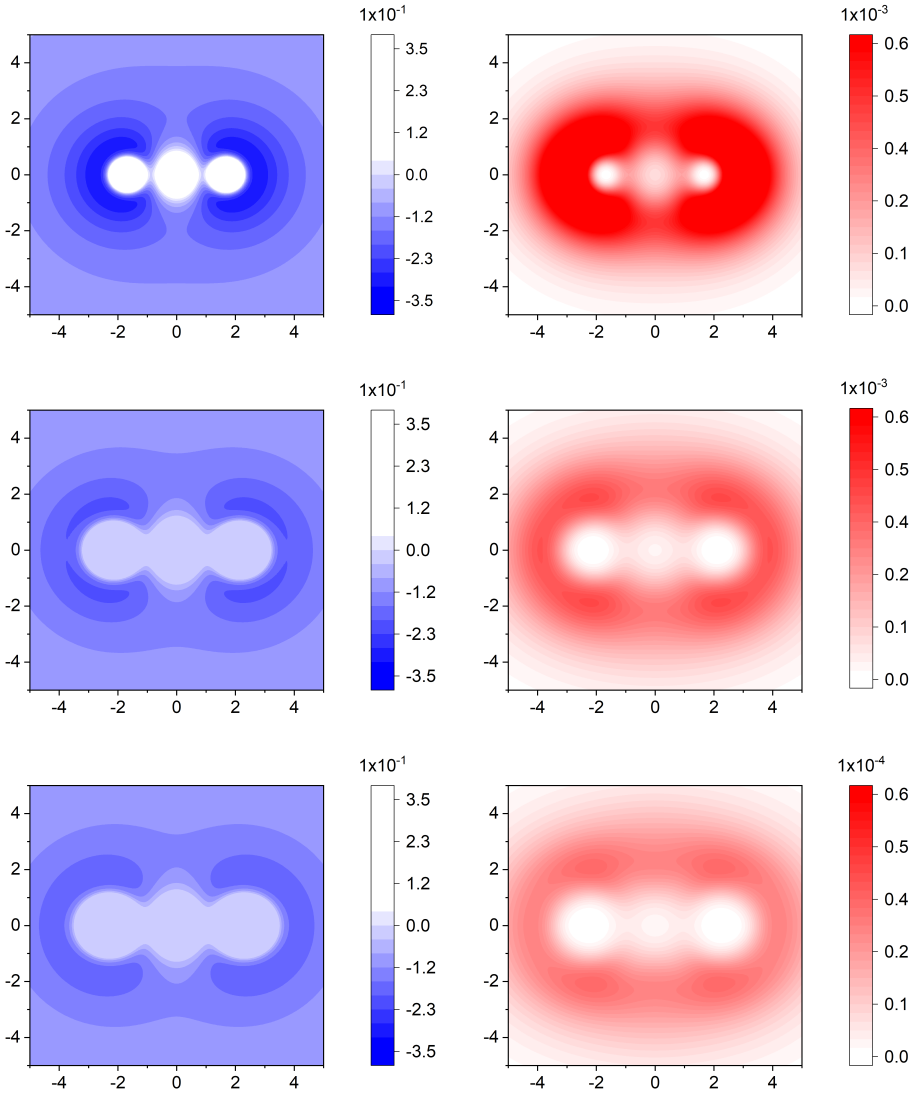

Figure S2 Top left : ESP of LiF_2^-, Middle left: ESP of $LiCl_2^-$, Bottom left: ESP of $LiBr_2^-$. Top right: positron density of $PsLiF_2$, Middle right: positron density of $PsLiCl_2$, Bottom right: positron density of $PsLiBr_2$.

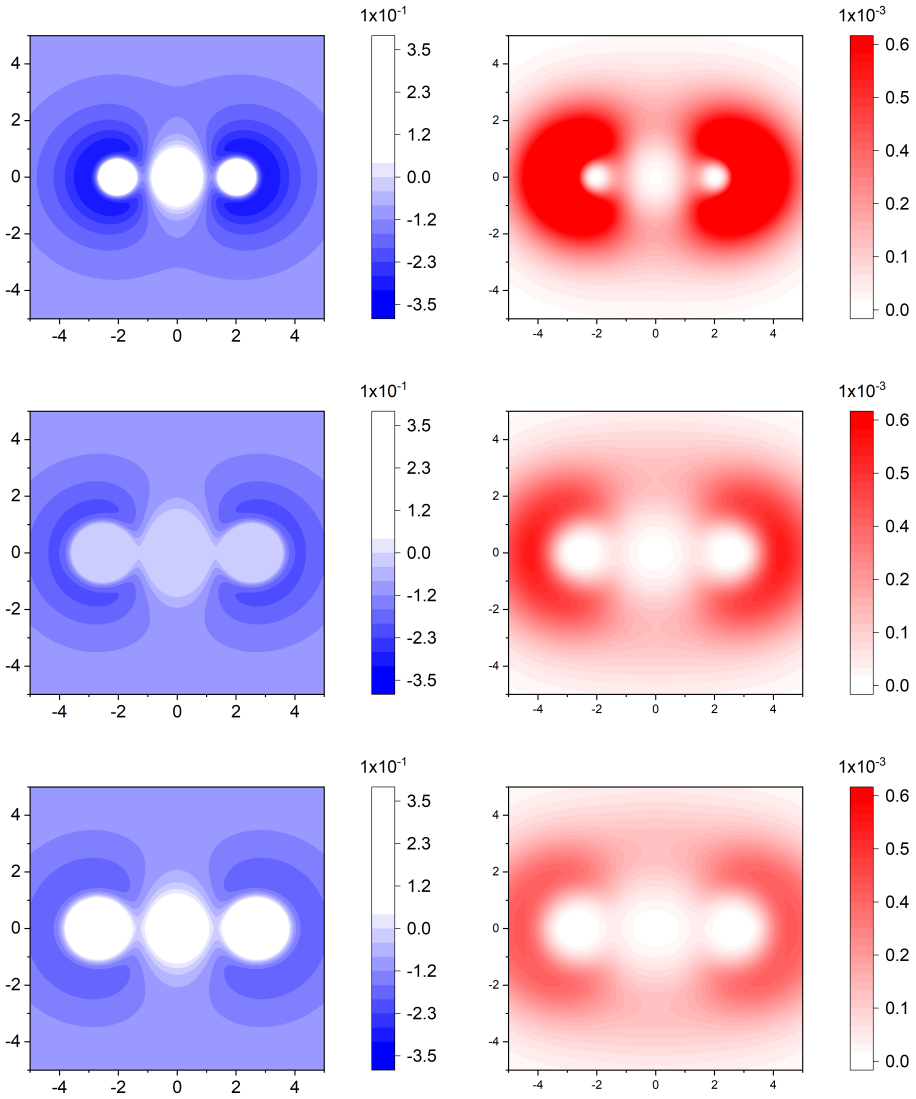

Figure S3 Top left : ESP of NaF_2^-, Middle left: ESP of $NaCl_2^-$, Bottom left: ESP of $NaBr_2^-$. Top right: positron density of $PsNaF_2$, Middle right: positron density of $PsNaCl_2$, Bottom right: positron density of $PsNaBr_2$.

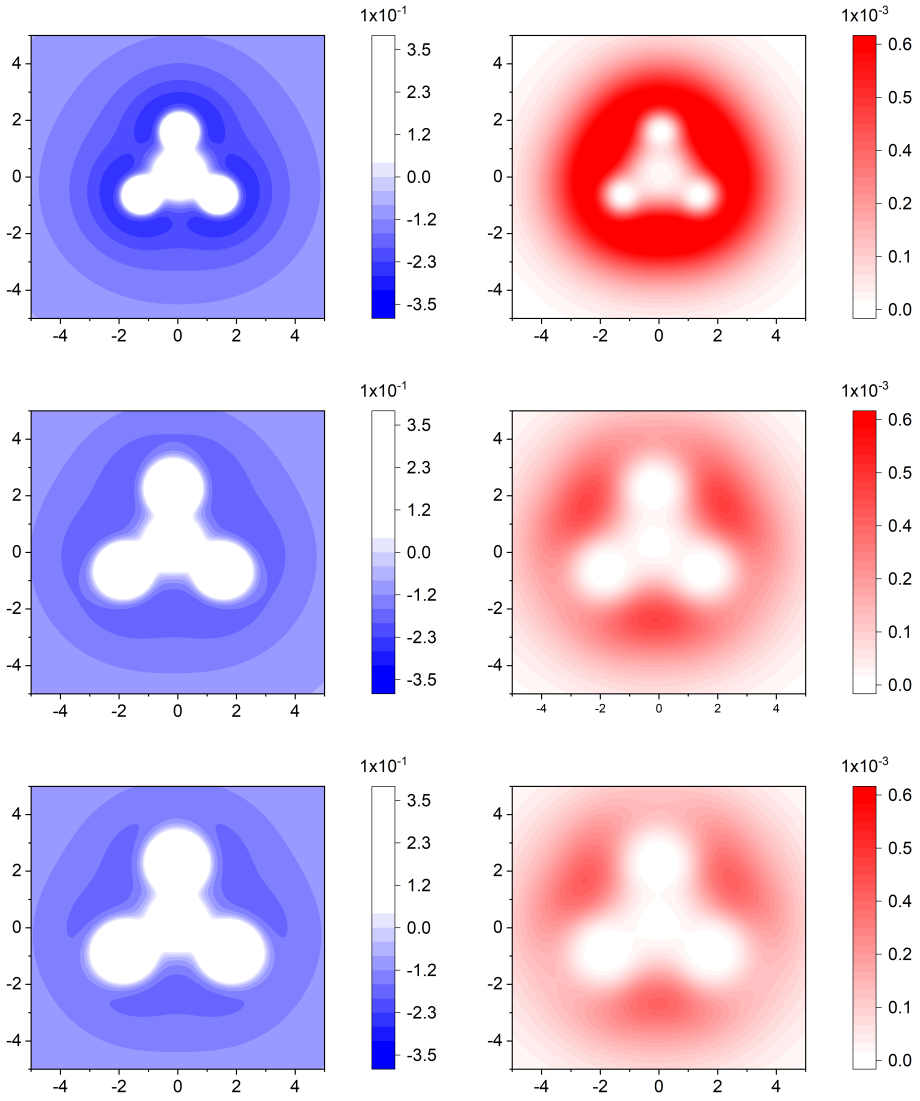

Figure S4 Top left : ESP of BeF_3^-, Middle left: ESP of $BeCl_3^-$, Bottom left: ESP of $BeBr_3^-$. Top right: positron density of $PsBeF_3$, Middle right: positron density of $PsBeCl_3$, Bottom right: positron density of $PsBeBr_3$.

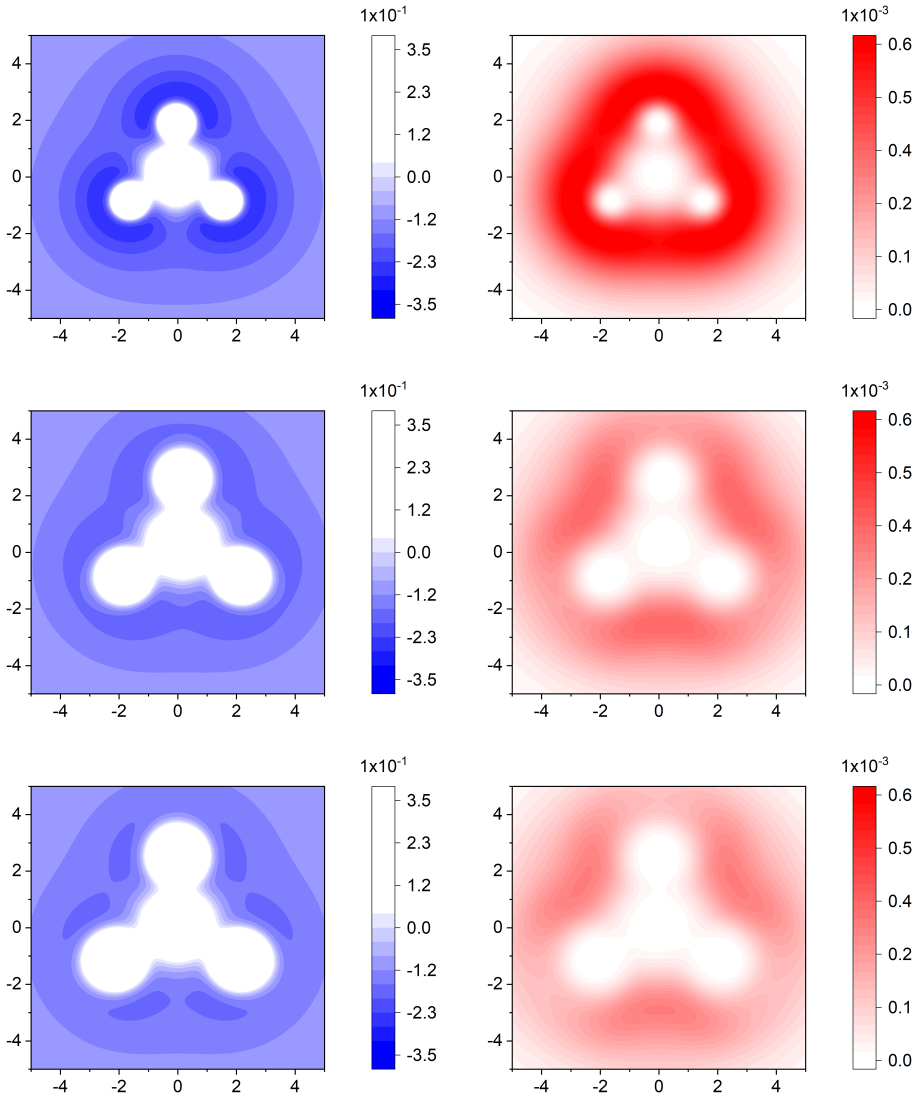

Figure S5 Top left : ESP of MgF_3^-, Middle left: ESP of $MgCl_3^-$, Bottom left: ESP of $MgBr_3^-$. Top right: positron density of $PsMgF_3$, Middle right: positron density of $PsMgCl_3$, Bottom right: positron density of $PsMgBr_3$.

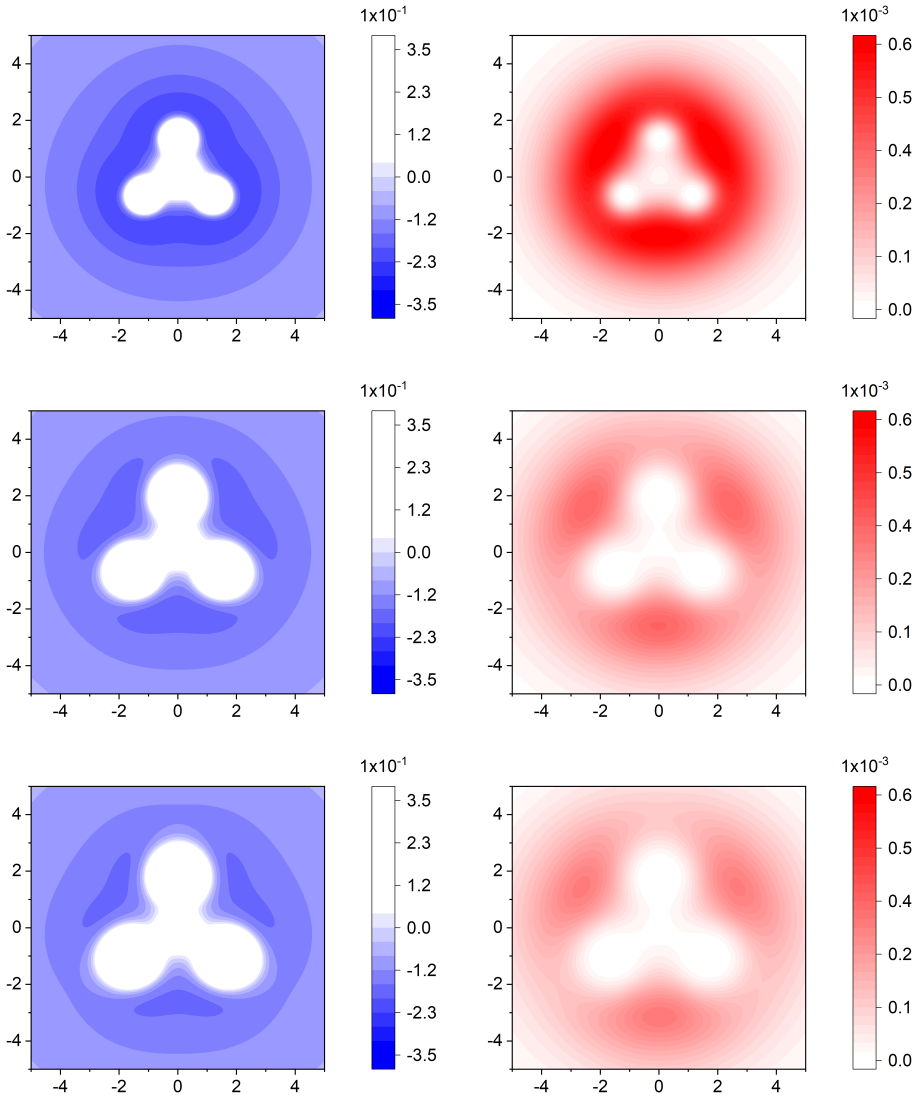

Figure S6 Top left : ESP of BF_4^-, Middle left: ESP of BCl_4^-, Bottom left: ESP of BBr_4^-. Top right: positron density of $PsBF_4$, Middle right: positron density of $PsBCl_4$, Bottom right: positron density of $PsBBr_4$.

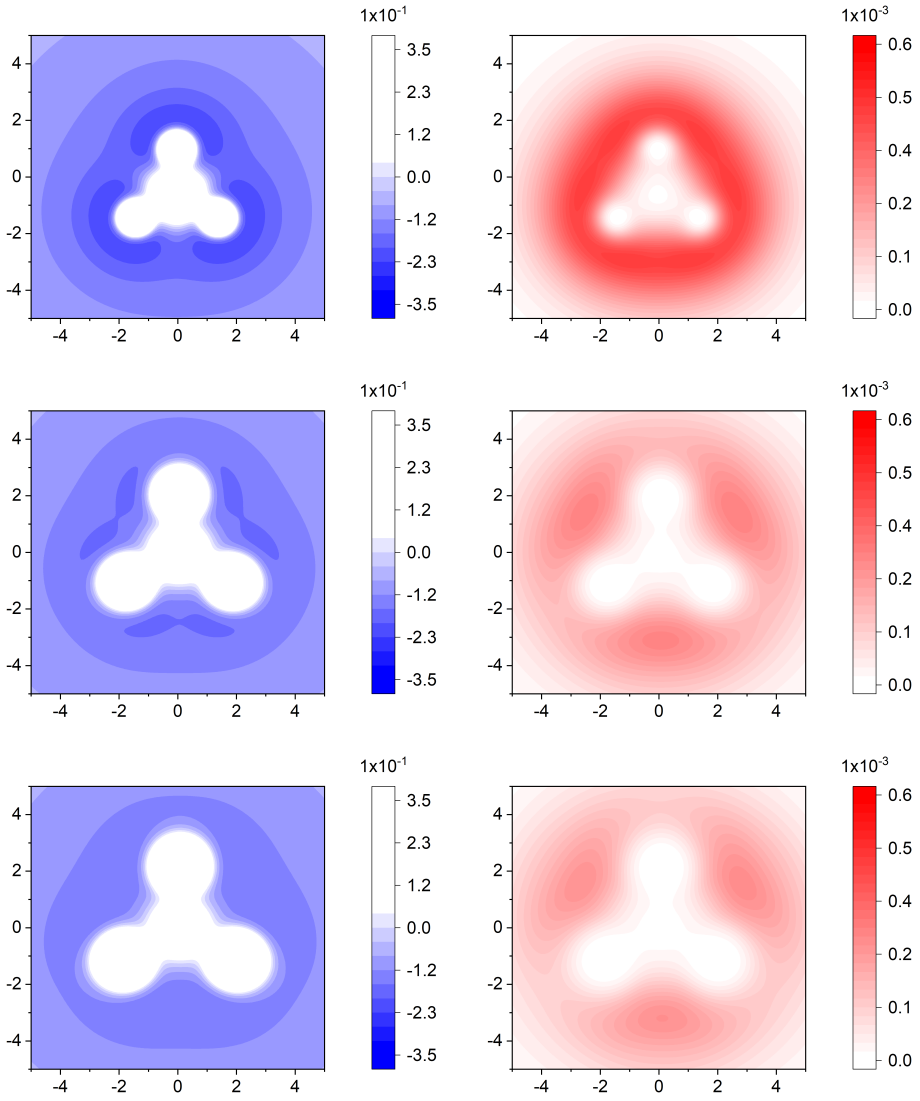

Figure S7 Top left : ESP of AlF_4^-, Middle left: ESP of $AlCl_4^-$, Bottom left: ESP of $AlBr_4^-$. Top right: positron density of $PsAlF_4$, Middle right: positron density of $PsAlCl_4$, Bottom right: positron density of $PsAlBr_4$.

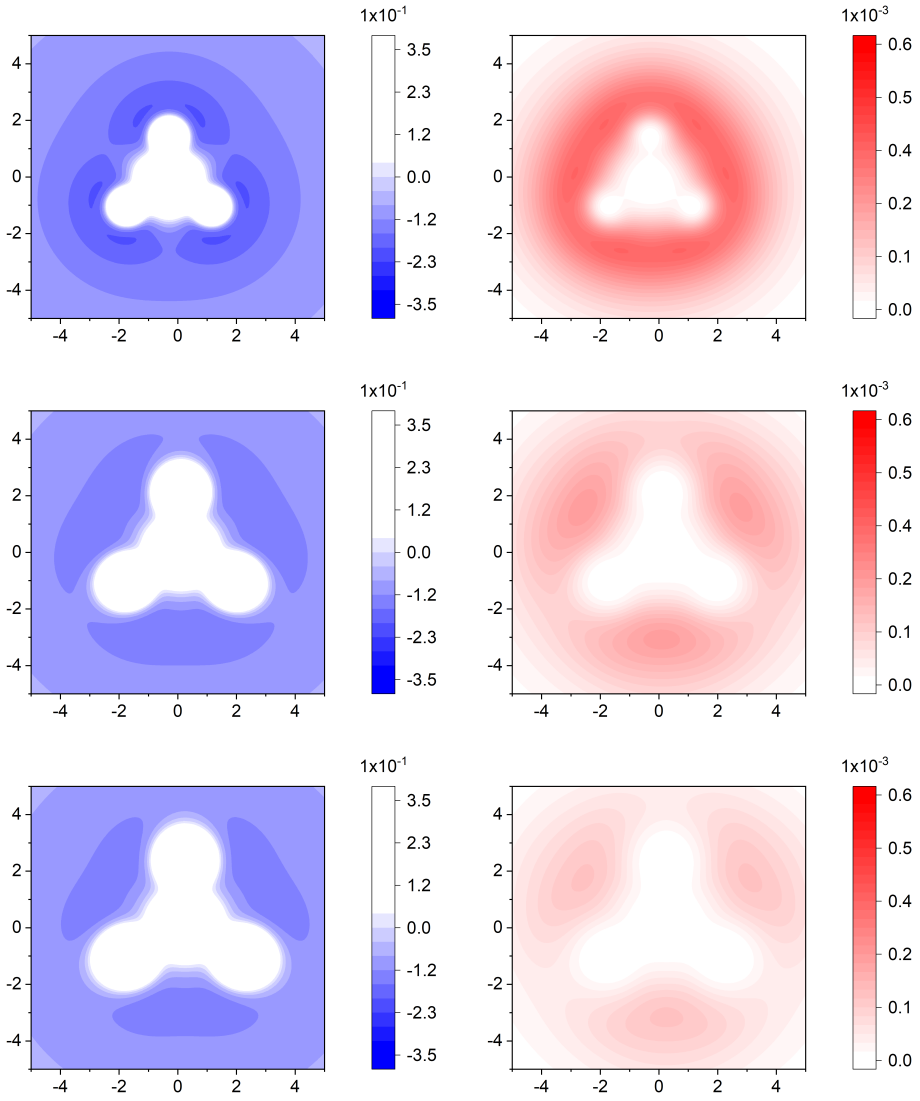

Figure S8 op left : ESP of SiF_5^-, Middle left: ESP of $SiCl_5^-$, Bottom left: ESP of $SiBr_5^-$. Top right: positron density of $PsSiF_5$, Middle right: positron density of $PsSiCl_5$, Bottom right: positron density of $PsSiBr_5$.

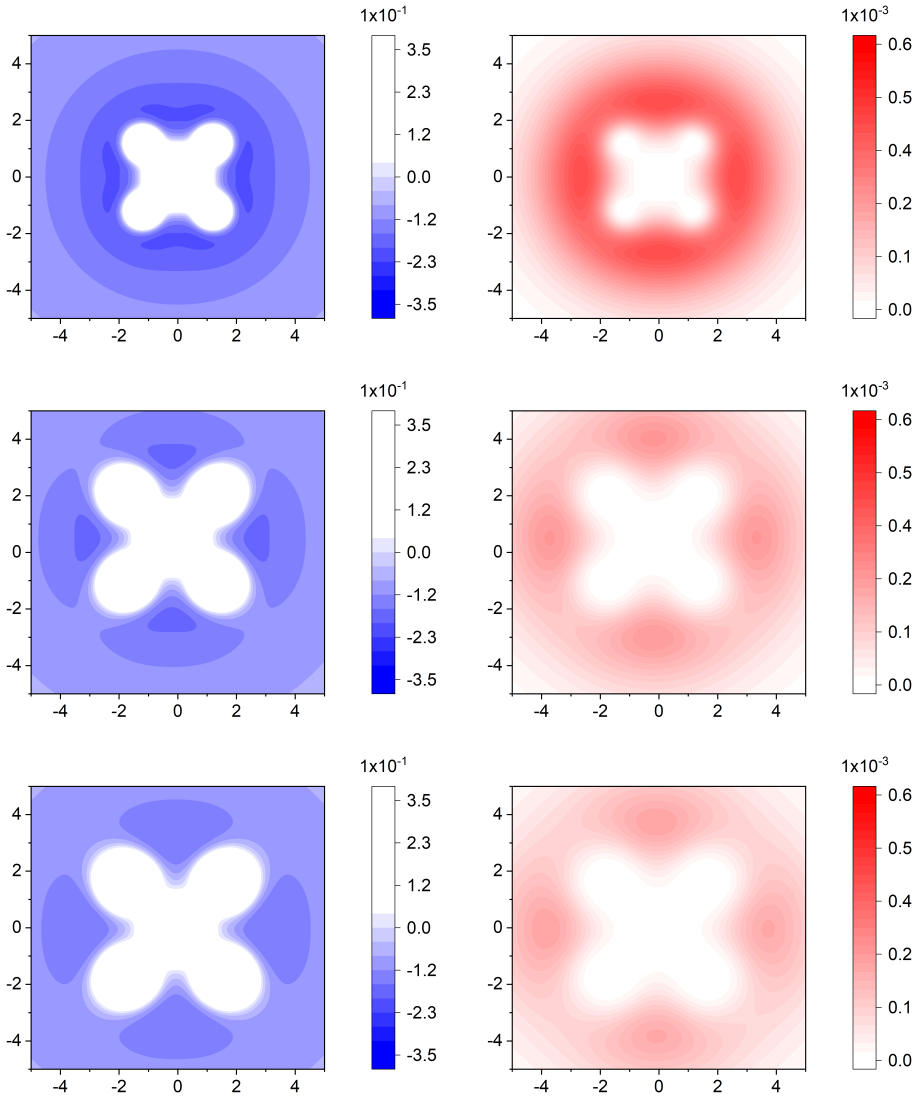

Figure S9 Top left : ESP of PF_6^-, Middle left: ESP of PCl_6^-, Bottom left: ESP of PBr_6^-. Top right: positron density of $PsPF_6$, Middle right: positron density of $PsPCl_6$, Bottom right: positron density of $PsPBr_6$.

References

[1] G. L. Gutsev, P. Jena and R. J. Bartlett, *Chem. Phys. Lett.*, 1998, **292**, 289–294.